

HOSTED BY



Contents lists available at ScienceDirect

## International Journal of Veterinary Science and Medicine

journal homepage: [www.elsevier.com/locate/ijvsm](http://www.elsevier.com/locate/ijvsm)  
[www.vet.cu.edu.eg](http://www.vet.cu.edu.eg)

Full Length Article

Antibacterial effect of gold nanoparticles against *Corynebacterium pseudotuberculosis*Marwah M. Mohamed<sup>a</sup>, Shereen A. Fouad<sup>a</sup>, Hisham A. Elshoky<sup>b</sup>, Gina M. Mohammed<sup>c</sup>,  
Taher A. Salaheldin<sup>b,d,\*</sup><sup>a</sup> Department of Bacterial Diagnostic Products, Veterinary Serum and Vaccine Research Institute, Egypt<sup>b</sup> Nanotechnology and Advanced Material Central Lab, Agriculture Research Center, Egypt<sup>c</sup> Central Laboratory for Evaluation Veterinary Biologics, Agriculture Research Center, Egypt<sup>d</sup> Mostafa Elsayed Nanotechnology Research Centre, British University in Egypt, Egypt

## ARTICLE INFO

## Article history:

Received 4 January 2017

Revised 3 February 2017

Accepted 13 February 2017

Available online 28 April 2017

## Keywords:

*C. pseudotuberculosis*

Gold nanoparticles

Laser

Antibacterial agent

Caseous lymphadenitis

Sheep and goats

## ABSTRACT

*Corynebacterium pseudotuberculosis* is the etiological agent of chronic caseous lymphadenitis. The bacterium infects goats and sheep causing great economic loss worldwide annually. The present work aims to evaluate the efficiency of gold nanoparticles (AuNPs) and AuNPs – laser combined therapy as antibacterial approaches against *C. pseudotuberculosis* bacteria *in vitro*. Gold nanoparticles 25 nm were synthesized by co-precipitation method and characterized by different techniques including; Transmission Electron Microscope (TEM), X-ray Diffraction and Dynamic Light Scattering. Three concentrations of AuNPs (50, 100 and 200 µg/mL) were utilized for estimating the bacterial growth rate and the Minimum Inhibitory Concentration (MIC). The mechanism of interaction between AuNPs and bacteria was evaluated by transmission electron microscopic image analysis. Confocal Laser Scanning Microscopic technique was used to study the cytotoxic action of AuNPs and laser against *C. pseudotuberculosis*. Results revealed that MIC of AuNPs and AuNPs – laser combined therapy were 200 µg/mL and 100 µg/mL respectively. TEM image analysis illustrated that gold nanoparticles penetrated the thick wall of *C. pseudotuberculosis* and accumulated as intracellular agglomerates. Laser light enhanced the antimicrobial activity of gold nanoparticles by at least one fold due to its photo thermal combined effect that might be used as an effective antibacterial approach against *C. pseudotuberculosis*.

© 2017 Faculty of Veterinary Medicine, Cairo University. Production and hosting by Elsevier B.V. This is an open access article under the CC BY-NC-ND license (<http://creativecommons.org/licenses/by-nc-nd/4.0/>).

## 1. Introduction

Caseous lymphadenitis (CLA) is one of the most sporadic chronic bacterial origin disease, infects mainly goats and sheep caused by *C. pseudotuberculosis*. This organism is gram positive, non-spore and facultative anaerobic rod shaped bacteria, several of which are pathogenic for man and animals. As long as the animal becomes infected with *C. pseudotuberculosis*, it survives and replicates within cells of the immune system that normally be the defense system against it and once the disease established, CLA is difficult to eradicate [1–3].

Most of the therapeutic routs are futile even the chemotherapeutic one that is because of the thick capsule that surrounds the abscesses of *C. pseudotuberculosis* [4]. Although the vaccination against *C. pseudotuberculosis* with dead bacteria or with an excreted proteins provides limited protection, the need for anti-genic compounds that can activate both humeral and cellular arms of the immune system is still the demand [5]. However, such methods are hard to achieve and hence limited effectiveness.

Nanomaterials became a promising and efficient candidate that can replace conventional materials with most applications in all fields of science and technology. As a result of the ultra-small size of nanomaterials that have higher surface to volume ratio and increased number of active atoms at their outer surfaces [6]. Some metallurgic nanomaterials have been approved as bactericidal and bacteriostatic agents, among those used are silver, gold and zinc, each with different properties and spectrum activities [7,8]. Gold nanoparticles (AuNPs) are widely used in enormous biological applications mainly in medical and gene therapy and biosensors for diagnosis. AuNPs are easy to prepare by co-precipitation

Peer review under responsibility of Faculty of Veterinary Medicine, Cairo University.

\* Corresponding author at: Mostafa Elsayed Nanotechnology Research Centre, British University in Egypt, El Sherouk City, and Suez Desert Road, Cairo 11837, P.O. Box 43, Egypt.

E-mail addresses: [Taher.salah@bue.edu.eg](mailto:Taher.salah@bue.edu.eg), [T1salah@hotmail.com](mailto:T1salah@hotmail.com) (T.A. Salaheldin).  
URL: <http://www.bue.edu.eg> (T.A. Salaheldin).

<http://dx.doi.org/10.1016/j.ijvsm.2017.02.003>

2314–4599/© 2017 Faculty of Veterinary Medicine, Cairo University. Production and hosting by Elsevier B.V.  
This is an open access article under the CC BY-NC-ND license (<http://creativecommons.org/licenses/by-nc-nd/4.0/>).

approach and may have lower toxicity compared to other metallic nanomaterials such as silver nanoparticles [9]. The problem of antibiotic resistant bacteria and their emphasis on health care costs, that encourages researchers to innovate new approaches to develop more effective antimicrobial agents to overcome the bacterial resistance and reduce their cost [10]. One approach being tested is photodynamic therapy (PDT), which uses light absorbing dyes to generate toxic oxygen radicals to kill the bacteria. However, this treatment might not be effective for infections in hypoxic environments. Another promising approach is to use metal nanoparticles, and laser energy to physically damage the bacteria through Photo Thermal Therapy (PTT) [11]. The optical properties of conductive nanoparticles (NPs), such as those made of gold have been associated with the Surface Plasmon Resonance (SPR), which when confined to small colloids, is referred to as the localized surface plasmon resonance (LSPR). This phenomenon, in which the surface electrons oscillate collectively when irradiated with particular light energy resonated with its LSPR, causes wavelength dependent photo thermal effect. When gold NPs absorb resonating light energy, they release heat in accordance, making them useful in photo thermal therapy applications such as targeting cancer and bacterial cells. Laser-induced photothermal phenomena induce physical disruption of the bacterial cells leading to death [12]. The purpose of this study is to evaluate the efficiency and mechanism of the antimicrobial activity of gold nanoparticles (AuNPs) and AuNPs–laser combined therapeutic approach against *C. pseudotuberculosis* bacteria.

## 2. Materials and methods

### 2.1. Synthesis of gold nanoparticles (AuNPs)

Gold nanoparticles colloidal solution ( $25 \pm 5$  nm) was synthesized by co-precipitation protocol through the reduction of Gold Chloride hydrate ( $\text{HAuCl}_4$ ) (99.99%, Aldrich, USA) with Sodium citrate tribasic dihydrate (99%, Aldrich, USA) under boiling conditions [13]. All glass wears were cleaned and sterilized by aqua regia and dried in oven dryer at  $120^\circ\text{C}$ . DNA free deionized water (Millipore, USA) was used for preparation and dilutions. Fifty mL (0.03 mM)  $\text{HAuCl}_4$ , in 250 mL beaker, was brought to boil under stirring for 5 min. Sodium citrate tribasic dihydrate (0.5 mL) 1% solution was added at once under continuous stirring. The solution color turned bright red forming gold nanoparticles colloid, then left to cool and proceed for physicochemical characterization.

### 2.2. Characterization of gold nanoparticles

The characteristic SPR of AuNPs was recorded by absorption spectroscopic technique using a double beam UV–Vis–NIR spectrophotometer (Cary 5000, Agilent, UK) within the scanning range of 200–800 nm. Actual morphology of the prepared gold nanoparticles was imaged by High Resolution Transmission Electron Microscope (HR-TEM) operating at an accelerating voltage of 200 kV (Tecnai G2, FEI, Netherlands). Diluted colloidal gold nanoparticles solution was ultra-sonicated for 5 min to reduce the particles aggregation. Using micropipette, three drops from the sonicated solution were deposited on carbon coated-copper grid and left to dry at room temperature. HR-TEM images of the gold nanoparticles that deposited on the grid were captures for morphological evaluation. Dynamic Light Scattering (DLS) technique was utilized to estimate the average particle size distribution that was measured by zeta sizer (Malvern, ZS Nano, UK). The chemical structure of prepared gold nanoparticles was assessed using X-ray Diffraction (XRD) technique. Colloidal gold solution was centrifuge at 18,000 rpm for 30 min using cooling centrifuge,

the precipitated reddish brown pellet was dried in vacuum oven for 2 h then grinded into fine powder to be bombarded by X-ray for phase analysis. The corresponding XRD pattern was recorded in the scanning mode (X'pert PRO, PAN analytical, Netherlands) operated by Cu K radiation tube ( $=1.54 \text{ \AA}$ ) at 40 kV and 30 mA. The obtained diffraction pattern was interpreted by the standard ICCD library installed in PDF4 software. Qualitative and quantitative measurements of the applied gold nanoparticles concentrations were determined by Inductivity Coupled Plasma (ICP) technique (PerkinElmer ICP-OES: Optima 2000, Germany). Synthesis and characterization of gold nanoparticles were performed in Nanotechnology & Advanced Materials Central Laboratory, Agriculture Research Center, Egypt.

### 2.3. Strain and growth culture

For study the antibacterial activity of Au NPs on *C. pseudotuberculosis*, a local strain was isolated from lymph nodes of a native sheep suffered from caseous lymphadenitis, it was identified morphologically, biochemically and biologically at Bacterial Diagnostic Products, Veterinary Serum and Vaccine Research Institute, Cairo, Egypt. Brain heart infusion broth (DIFCO, Detroit, Mich., USA) and Brain heart infusion agar (DIFCO, Detroit, Mich., USA) were used as culture media [14,15]. The growth culture was performed using single colony of fully identified *C. pseudotuberculosis* bacteria field strain, it was picked up and inoculated into 100 mL of brain heart infusion broth then incubated at  $37^\circ\text{C}$  for 48 h. Serial dilutions were carried out using broth media to give a final organism density of  $10^5$  CFU/mL.

### 2.4. The antimicrobial activity of AuNPs

The Minimum Inhibitory Concentration (MIC) of three different concentrations of AuNPs (50, 100 and 200  $\mu\text{g/mL}$ ) was determined using the plate count method [16,17]. Twenty mL from the previously prepared culture medium (containing  $10^5$  CFU/mL of bacterial cells) was a liquated into four tubes (5 mL each), then the Au NPs were added in each tubes in the following concentration 0, 50, 100 and 200  $\mu\text{g/mL}$ , respectively. The tubes were incubated in a shaking incubator at  $37^\circ\text{C}$  for 24 h. After incubation, 50  $\mu\text{L}$  from each tube was spread onto brain heart infusion agar and incubated at  $37^\circ\text{C}$  for 24 h; the numbers of colonies growing on agar were estimated. Measurements of the optical density (O.D.) at 600 nm of the treated bacteria were graphed to estimate the growth curves [10].

### 2.5. Laser induced gold nanoparticles antibacterial effects

The MIC for 3 groups was performed from a mixture of culture media and Au NPs (0, 50, 100 and 200  $\mu\text{g/mL}$ ) [16,17], the culture tubes were incubated in a shaking incubator at  $37^\circ\text{C}$  for 24 h. Incubation tubes were subjected to 520 nm laser light, 20 mW, at different exposure time (5, 10 and 20 min.) for each group, respectively. Fifty  $\mu\text{L}$  from each culture tube were spread onto brain heart infusion agar and incubated at  $37^\circ\text{C}$  for 24 h; the numbers of colonies growing on agar were estimated. Measurements of the O.D. at 600 nm of the treated bacteria were graphed to estimate the growth curves [10].

### 2.6. AuNPs antibacterial mode of action

Electron microscope imaging and EDX analysis were performed to study the effect of AuNPs on the bacterial cell integrity and to elucidate whether the mode of action either extra or intra cellular. Culture treated with different concentrations of AuNPs and non-treated one of *C. pseudotuberculosis* were proceeded for fixation

process and sectioned as the following; bacteria were fixated in fixation solution (2% glutaraldehyde + 2% paraformaldehyde dissolved in 0.12 M Sorensen's buffer, pH 7.4) and then stained by (2%) Osmium Tetroxide solution for 1 h at 4°C. Embedding sections were cut on a MT6000 ultra microtome (Sorvall, New Castle, DE). Thin sections (0.1–0.05 mm) were examined and photographed using electron microscope (Tecnai G2, FEI, Netherlands) [11].

### 2.7. Confocal Laser Scanning image

Confocal Laser Scanning Microscopic (CLSM) (710, Carrel Zeiss, Germany) was used to study the antibacterial action of AuNPs on *C. pseudotuberculosis* bacteria at gold concentrations of 50, 100 and 200 µg/mL, for discrimination of live from dead cells on the basis of membrane integrity. Acridine Orange fluoresces green (AO) (sigma-Aldrich, USA) was used to stain live cells while Ethidium Bromide fluoresces red (EB) (sigma-Aldrich, US) was used to stain dead cells. In brief, 20 µL of *C. pseudotuberculosis* bacteria before and after treatment (AuNPs and Laser) were placed in glass bases plates and 5 µL of AO/EB (1 mg/mL, 0.3 mg/mL, respectively) were added and left for 5 min, then the samples have been examined immediately under confocal microscopy before leakage of dyes from cells after five minutes. Microscopic inspection of the tested bacteria was carried out using the excitation laser lines at 405/530 and 543/640 nm [18].

## 3. Results

### 3.1. Characterization of gold nanoparticles

Fig. 1 shows physicochemical characterization of the synthesized gold nanoparticles to evaluate its properties using different techniques. Colloidal solution of spherical gold nanoparticles had a distinct bright red color and corresponding characteristic Surface Plasmon Resonance (SPR) absorption peak at 524 nm with Gaussian distribution curve, as indicated in Fig. 1A. For nanoparticle morphology and size determination, HR-TEM electrograph showed well uniformed spheres with average size of 25 ± 5 nm. The corresponding TEM diffraction pattern inset showed formation of gold nanoparticles with cubic crystal structure, Fig. 1B. Fig. 1C represents

the particle size distribution curve obtained from DLS measurements with excellent polydispersity index (PDI) 0.106. The measurement of the gold nanoparticles surface charge, zeta potential, was (−39 mV) as measured by DLS technique. Gold nanoparticles phase formation was tested by XRD analysis, Fig. 1D, based on Bragg's reflections low. Characteristic diffraction pattern showed sharp intense and narrow peaks at 38.14°, 44.39°, 64.61°, 77.58° and 81.13° 2θ angles those corresponding to *hkl* parameters of (111), (200), (220), (311) and (222), respectively. The obtained diffraction pattern was compared with the standard ICCD library installed in PDF4 software, card no: (04-003-3089).

### 3.2. Antibacterial activity of AuNPs/AuNPs-laser enhanced

The MIC of AuNPs against *C. pseudotuberculosis* was 200 µg/mL Fig. 2. While the MIC of AuNPs-laser Enhanced was recorded to be 100 µg/mL. Fig. 2 illustrates a comparative study between the uses of AuNPs alone as antibacterial active agent against *C. pseudotuberculosis* bacteria and AuNPs-laser combined therapy. Laser enhancement depended upon the exposure time. For dose of 50 µg/mL AuNPs, the inhibition of the bacterial growth was 75%, 85% and 95% for exposure time of 5 min, 10 min and 20 min, respectively, as clearly recorded in the corresponding growth curves.

### 3.3. AuNPs antibacterial mode of action

The morphological changes of bacterial cells represented information about the antibacterial mode of action of gold nanoparticles either extracellular or intracellular. High Resolution Transmission Electron Microscope (HRTEM) imaging of AuNPs and AuNPs-laser treated *C. pseudotuberculosis* bacteria compared to the untreated control one. Fig. 3A shows HR-TEM image of treated bacteria, it was observed that gold nanoparticles were capable to penetrate the thick cell wall of *C. pseudotuberculosis* bacteria suggesting the intracellular mechanism of action. Energy Dispersive X-ray (EDX) analysis of the imaged sample confirmed the formation of gold aggregates inside the cytoplasm as shown in Fig. 3B. The cell wall of control group was appeared intact, however, vacuoles formed inside the bacterial cells treated with AuNPs, while

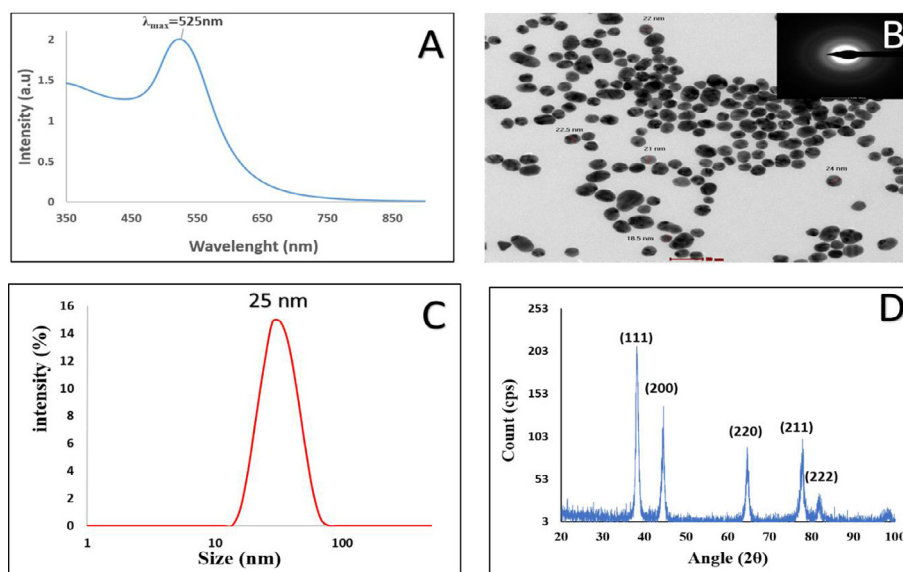


**Fig. 1.** Characterization of gold nanoparticles (AuNPs). (A): Absorption spectrum of gold nanoparticles. (B): HRTEM image showing spherical shape of prepared gold nanoparticles with average size 25 nm. (C): Particle size distribution of prepared gold nanoparticles showing the average size of 25 nm. (D): XRD pattern analysis indicating the formation of gold nanoparticles with cubic unit crystal.

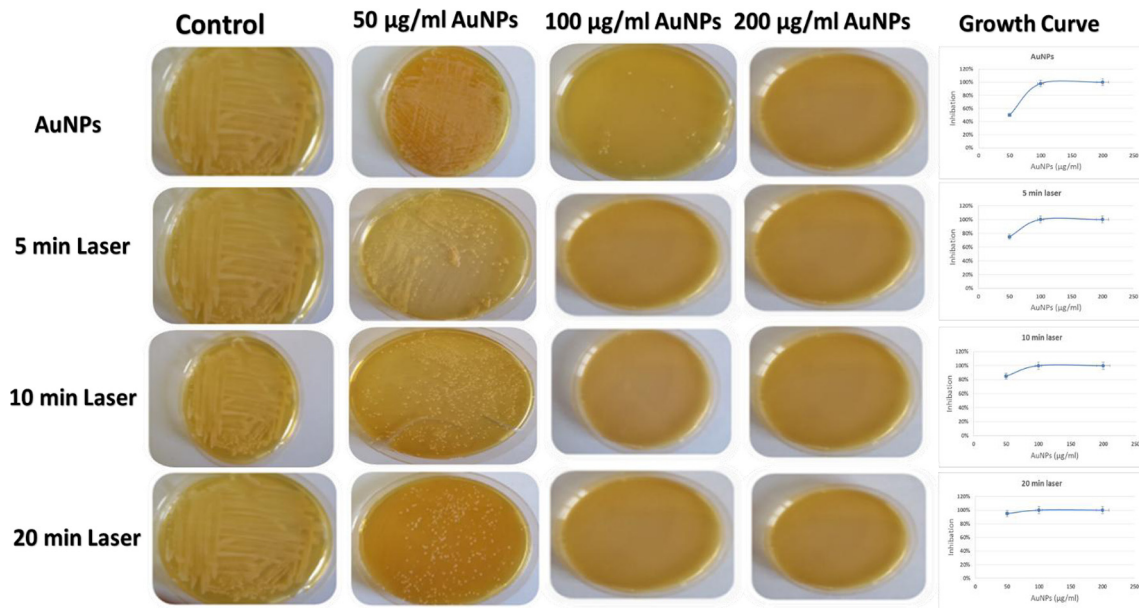


**Fig. 2.** Antibacterial activity of AuNPs and Laser induced AuNPs against *C. pseudotuberculosis* at different gold concentration (0, 50, 100 and 200 µg/ml) and different laser exposure times (5, 10 and 20 min). Plates represent the plate count method describing the number of growth colonies and the growth curves represent the percentage of inhibition rate of all treatments.

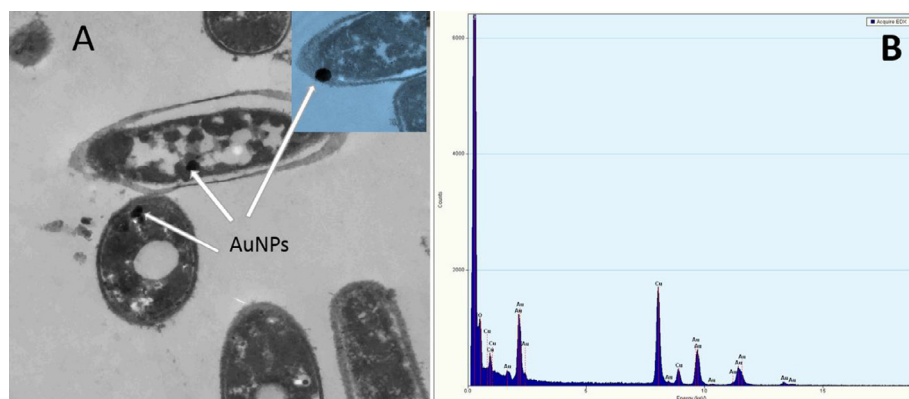


**Fig. 3.** HR-TEM electrograph of intracellular localization of gold nanoparticles within *C. pseudotuberculosis* bacteria, (A): penetration of AuNPs into the cell wall and accumulation in cytoplasm by HR-TEM. (B): Energy Dispersive X-ray (EDX) image analysis of the intracellular AuNPs aggregates.

complete destruction was recorded within bacteria exposed to combined AuNPs–Laser treatment. As clearly illustrated in Fig 4.

### 3.4. Confocal Laser Scanning Microscopic imaging

Confocal Laser Scanning Microscopic (CLSM) imaging of *C. pseudotuberculosis* (treated with both AuNPs and AuNPs–Laser) stained with Acridine orange (AO) fluoresces green (stain life cells) and Ethidium bromide (EB) fluoresces red (stain dead cells) which used for visual differentiation between live and dead cells based on membrane integrity. Fig. 5 represents the distribution of dead/viable bacteria in the gold nanoparticles co-culture tested concentrations (0, 50 µg/mL, 100 µg/mL and 200 µg/mL AuNPs), where in Fig. 5A, only live bacteria appear in green fluorescence which is corresponding to the control untreated bacteria. Fig. 5B represents the 50 µg/mL AuNPs treatment, the viability was about 50% that is why yellowish orange fluorescence due to the cross over between the green (live cells) and red (dead cells). The viability was zero for concentrations of 100 µg/mL and 200 µg/mL AuNPs, only red fluorescence appeared as a result of dead abundance, (Fig. 5C and D).

With the same extent, CLSM imaging of the combined treatment (AuNPs–Laser), Fig. 6 represents the distribution of dead/viable bacteria in the AuNPs–Laser (5 min laser exposure) co-culture tested concentrations (0, 50 µg/mL, 100 µg/mL and 200 µg/mL AuNPs). Where in Fig. 6A, the control untreated live bacteria appeared in green fluorescence. Fig. 6B represents the 50 µg/mL AuNPs–Laser treatment, the viability was about 50% that is why yellowish orange fluorescence due to the cross over between the green (live cells) and red (dead cells). The viability was zero for concentrations of 100 µg/mL and 200 µg/mL AuNPs–Laser, where red fluorescence appeared as a result of dead abundance, Fig. 6C and D. It is remarked from Fig. 6D that laser disintegrates the bacterial cells as a low number of dead cells appear.

## 4. Discussion

Nanotechnology has attracted global attention because nanoparticles have novel and unique properties from their bulk equivalents. The antibacterial activity of nanoparticles largely has been studied with human pathogenic bacteria, such as *E. coli* and

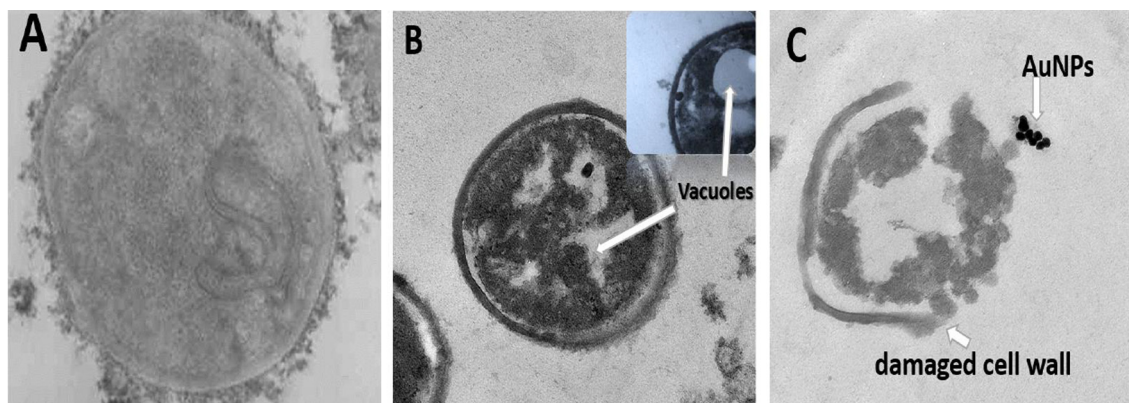


**Fig. 4.** Intracellular mode of action imaged by HR-TEM. (A): untreated bacterial cell. (B): AuNPs induce vacuole formation in cytoplasm. (C): AuNPs-laser induced cellular destruction.

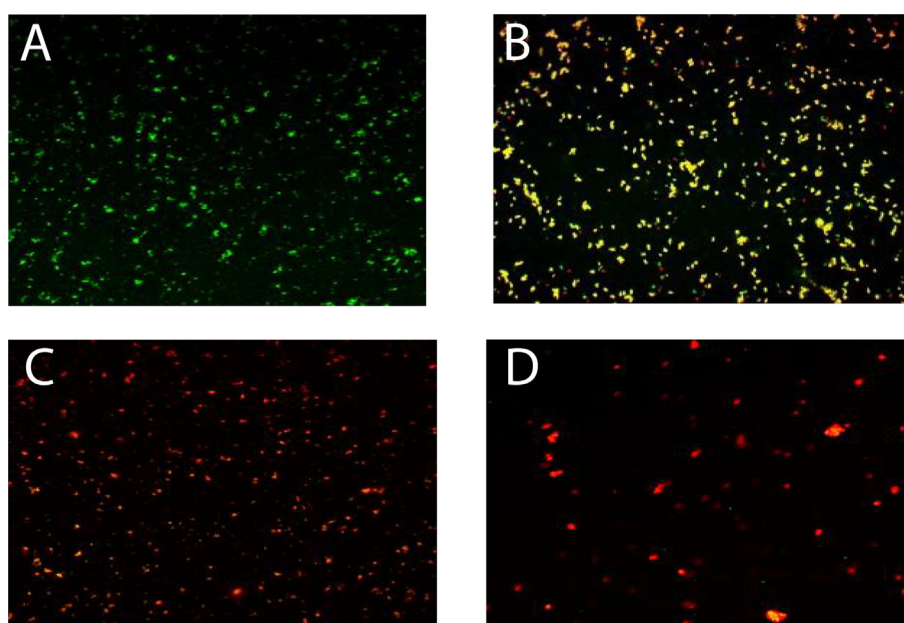


**Fig. 5.** CLSM images for viable/dead *C. pseudotuberculosis* bacteria in the AuNPs co-culture and stained with Acridine Orange (AO) green fluorescence and Ethidium Bromide (EB) red fluorescence.. (A) Deionized Water control; (B) 50 µg/mL AuNPs. (C) 100 µg/mL AuNPs; (D) 200 µg/mL AuNPs. Magnification, ×40.

*S. aureus* [10]. It has been reported that the biophysical interactions occur between NPs and bacteria through biosorption, aggregation, and cellular uptake causing membrane damage and toxicity. Still a comprehensive understanding of antibacterial mechanisms is needed to improve the effectiveness of NPs in disease treatment [8].

In this investigation, the antibacterial effects of AuNPs on *C. pseudotuberculosis* was studied. Gold nanoparticles were synthesized using citrate reduction method that is an easier and rapid method with controlled size and shape [13]. The shape absorption peak with well performed Gaussian distribution implies uniformity of gold nanoparticles formation with no aggregation and perfect dispersion [19,20]. The average size of the synthesized AuNPs was  $25 \pm 5$  nm with spherical shape as illustrated by high resolution electron microscopic image and DLS measurement. The Low Polydispersity Index (PDI), 0.106, reflects monodispersity and perfect dispersion of the nanoparticles with no aggregation. The high electronegative value ( $-39$  mV) of zeta potential indicates high degree of gold nanoparticles colloidal stability and perfect capping effect of citrate ions and particle-particles repulsion that prevents the particles aggregation or precipitation [21]. For chemical struc-

ture analysis, XRD pattern confirms the phase formation of gold nanoparticles with face-centered cubic crystal structure.

The MIC is relatively high compared to previous published work that studying the bactericidal effect of gold nanoparticles against the different bacterial stains such as *K. pneumoniae*, *S. typhi*, *P. aeruginosa* and *E. coli*, where MICs ranged from 20 to 40 µg/mL. the reason might be attributed to the thicker wall of *C. pseudotuberculosis* bacteria that reduces the penetration rate of AuNPs through cell wall and hence reduces the antibacterial activity of AuNPs at lower concentrations. It is recorded that, the laser light enhances the antimicrobial activity of gold nanoparticles by at least one fold. This might be attributed to the photothermal effect resulting from the unique property of nano scaled gold colloidal solution that has strong enhanced absorption band at 524 nm corresponding to the AuNPs Surface Plasmon Resonance (SPR) oscillations. Upon exposure to resonating laser emission line, the kinetic energy of gold nanoparticles increases resulting in local heating of the exposed target which is the gold nanoparticles treated bacteria in the present experiment. The generated photothermal effect can be employed for rapid and efficient bacterial cell destruction [22–25]. Laser enhancement depends on the exposure time.

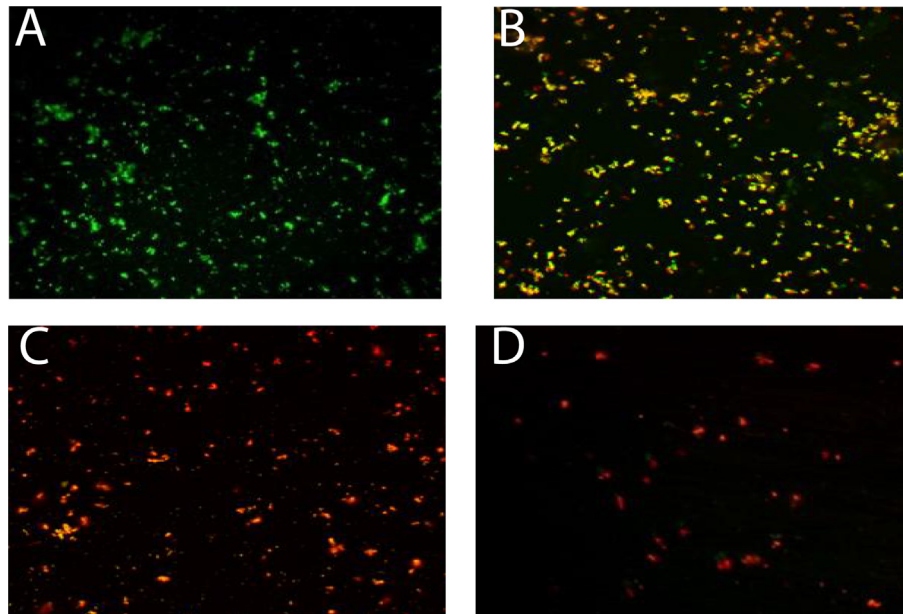


**Fig. 6.** CLSM images for viable/dead *C. pseudotuberculosis* bacteria in the AuNPs co-culture and stained with Acridine Orange (AO) green fluorescence and Ethidium bromide (EB) red fluorescence, staining. (A) Laser - deionized Water control; (B) 50 µg/mL AuNPs-Laser. (C) 100 µg/mL AuNPs-Laser; (D) 200 µg/mL AuNPs-Laser. Magnification, ×40.

Similar results were obtained from other studies, which showed that the laser enhanced nanoparticles applied to *S. aureus* reduced significantly the number of viable bacteria [26]. Zharov et al. [11] applied the combined triple approach, gold nanoparticles, laser and multifunctional photothermal microscope, for localized killing of *S. aureus* *in vitro* where photothermal bacterial damage accompanied by formation of bubble due to local overheating produced by gold nanoparticles upon absorbing the incident laser light energy, that transforms directly into heat energy [11].

The morphological changes of bacterial cells represent information about the antibacterial action mode of gold nanoparticles either extracellular or intracellular that imaged by HRTEM and by EDX. The suggested mechanism for antibacterial activity of the gold nanoparticles is attributed to generation of Reactive Oxygen Species (ROS) that causes increase of the oxidative stress of microbial cells and release of intracellular lactate dehydrogenase enzyme into extracellular medium in form of vacuole formation as an indication of potent activity [27–29]. Such effect was enhanced and exaggerated by photothermal degeneration in combined approach, AuNPs-laser, causes quick loss of cell membrane integrity [24].

The obtained results of Confocal Laser Scanning Microscopic (CLSM) imaging of *C. pseudotuberculosis* (treated with both AuNPs and AuNPs-Laser) came in accordance with the MIC data and transmission electron microscopic technique images. Laser disintegrates the bacterial cells as a low number of dead cells appeared. The present work recommends the use of CLSM technique as a rapid and accurate test for evaluating the efficacy of antimicrobial nanomaterials.

## 5. Conclusions

Although the thickness of the bacterial wall, gold nanoparticles induce intracellular antibacterial activity against *C. pseudotuberculosis* due to its ultra-fine size which facilitates its cellular penetration. The antibacterial activity of the gold nanoparticles might be attributed to generation of Reactive Oxygen Species (ROS) that causes increase of the oxidative stress of microbial cells in form of vacuole formation as an indication of potent activity. Such effect

was enhanced and exaggerated by photothermal degeneration in combined approach, AuNPs-laser, causing quick loss of cell membrane integrity. The laser light enhances the antimicrobial activity of gold nanoparticles by at least one fold. It could be concluded that the AuNPs combined with laser exposure can be used as local effective antibacterial approach for *C. pseudotuberculosis*.

## Competing interests

The authors of the present work report that there is no conflict of interest in this work.

## References

- [1] Paton MW, Mercy AR, Wilkinson FC, Gardner JJ, Sutherland SS, Ellis TM. The effects of caseous lymphadenitis on wool production and body weight in young sheep. *Aust Vet J* 1988;65:117–9.
- [2] Dorella FA, Pacheco LGC, Oliveira SC. *C. pseudotuberculosis*: microbiology, biochemical properties, pathogenesis and molecular studies of virulence. *Vet Rec* 2006;37:201–18.
- [3] Jesse FF, Adamu L, Osman AY, Fauzan BA, Haron AW, Saharee AA, et al. Polymerase chain reaction detection of *C. pseudotuberculosis* in the brain of mice following oral inoculation. *Inter J of Anim and Vet Adv* 2013;5:29–33.
- [4] Brown CC, Olande HJ, Biberstein EL, Morse SM. Use of a toxoid vaccine to protect goats against intradermal challenge exposure to *C. pseudotuberculosis*. *Am J Vet Res* 1986;47:1116–9.
- [5] Anderson M, Nairn ME. Control of Caseous Lymphadenitis in goats by vaccination. *Colloques de LINRA* 1984;28:605–9.
- [6] Azam A, Ahmed F, Arshi N, Chaman M, Naqvi AH. One step synthesis of gold nanoparticles and their antibacterial activities against *E. coli*. *Int J Theor Appl Sci* 2009;1:1–4.
- [7] Lansdown AB. Silver in health care: antimicrobial effects and safety in use. *Curr Probl Dermatol* 2006;33:17–34.
- [8] Zhou Y, Kong Y, Kundu S, Cirillo JD, Lian GH. Antibacterial activities of gold and silver nanoparticles against *E.coli* and *bacillus Calmette-Guérin*. *J Nanobiotechnol* 2012;10:19.
- [9] Shamaila S, Zafar N, Riaz S, Sharif R, Nazir J, Naseem S. Gold nanoparticles: an efficient antimicrobial agent against enteric bacterial human pathogen. *J Nanomaterials* 2016;6:71.
- [10] Soo- Hwan K, Lee H, Seon Ryu D, Choi SJ, Seok LD. Antibacterial activity of silver – nanoparticles against *S. aureus* and *E. coli*. *Korean J Microbiol Biotechnol* 2011;39:77–85.
- [11] Zharov VP, Mercer KE, Galitovskaya EN, Smeltzer MS. Photo thermal nano therapeutics and nano diagnostics for selective killing of bacteria targeted with gold nanoparticles. *Biophys J* 2006;90:619–27.

- [12] Millenbaugh NJ, DeSilva M, Baskin J, Elliot WR. Method of using laser induced optoacoustics for the treatment of drug resistant microbial infection. Patent Appl Pub 2014:1–5.
- [13] Frens G. Controlled nucleation for the regulation of the particle size in monodisperse gold suspensions. *Nature* 1973;241:20–2.
- [14] Quinn PJ, Carter ME, Markey BK, Carter GR. *Clinical veterinary microbiology*. London: Wolfe Publishing; 1994. p. 261–7.
- [15] Koneman EW, Allen SD, Danda MW, Soherchenberger PC, Winn WC. *Colour atlas and text book of diagnostic microbiology*. Fifth ed. Philadelphia, New York: Lippincott; 1997.
- [16] Magana SM, Quintana P, Aguilar DH, Toledo JA, Angeles-Chavez C, Cortes MA, et al. Antibacterial activity of montmorillonites modified with silver. *J. Mol Catal A Chem* 2008;281:192–9.
- [17] Wang JX, Wen LX, Wang ZH, Chen JF. Immobilization of silver on hollow silica nanospheres and nanotubes and their antibacterial effects. *Mater Chem Phys* 2006;96:90–7.
- [18] Kim BS, Oh JM, Kim KS. BSA-FITC-loaded microcapsules for in vivo delivery. *J biomaterials* 2009;30:902–9.
- [19] Aryal S, Bahadur KCR, Bhattarai SR, Prabu P, Kim HY. Immobilization of collagen on gold nanoparticles: preparation, characterization, and hydroxyapatite growth. *J Mater Chem* 2006;16:4642–8.
- [20] Perez-Juste J, Pastoriza-Santos I, Liz-Marzan L, Mulvaney P. Gold nanorods: synthesis, characterization and applications. *Coord Chem Rev* 2005;249:1870–901.
- [21] Horisberger M. Quantitative aspects of labelling colloidal gold with proteins in immunocytochemistry, in: Zulauf, M., Lindner, P., Terech, P. (Eds.), *Trends in Colloid and Interface Science IV SE - 32*, Progress in Colloid & Polymer Science. Steinkopff 1990; 156–60.
- [22] He X, Bischof JC. Quantification of temperature and injury response in thermal therapy and cryosurgery. *Crit Rev Biomed Eng* 2003;31:355–422.
- [23] Anderson RR, Parrish JA. Microvasculature can be selectively damaged using dye lasers: a basic theory and experimental evidence in human skin. *Lasers Surg Med* 1981;1:263–76.
- [24] Umamaheswari K, Baskar R, Chandru K, Rajendiran N, Chandirasekar S. Antibacterial activity of gold nanoparticles and their toxicity assessment. *BMC Inf Dis* 2014;14:64–75.
- [25] Guimaraes AS, Carmo FB, Pauletti RB, Seyffert N, Ribeiro D, Lage AP, et al. Caseous lymphadenitis: epidemiology, diagnosis and control. *Review Vet Microbiol* 2011;2:33–43.
- [26] Millenbaugh NJ, Baskin JB, DeSilva MN, Elliott WR, Glickman RD. Photothermal killing of *S. aureus* using antibody – targeted gold nanoparticles. *Inter J Nanomed* 2015;10:1953–60.
- [27] Brewer M, Zhang T, Dong W, Rutherford M, Tian ZR. Future approaches of nanomedicine in clinical science. *Med Clin North Am* 2007;91:963–1016.
- [28] Mishra A, Mehdi SJ, Irshad MD, Ali A, Sardar M, Moshahid M, et al. Effect of biologically synthesized silver nanoparticles on human cancer cells. *Sci Adv Mat* 2012;4:1200–6.
- [29] Zhang LW, Monteiro-Riviere NA. Use of confocal microscopy for nanoparticle drug delivery through skin. *J Biomed Optics* 2013;18(6):061214.